Luminance Adaptation Model for Increasing the Dynamic Range of an Imaging System Based on a CCD Camera

Marta de Lasarte,[1] Montserrat Arjona,[1] Meritxell Vilaseca,[1,] Francisco M. Martínez-Verdú,[2] and Jaume Pujol[1]

[1]*Centre for Sensors, Instruments and Systems Development (CD6), Technical University of Catalonia (UPC), Rambla Sant Nebridi 10, Terrassa, Barcelona 08222, Spain*

[2]*Department of Optics, University of Alicante (UA), Ap. Correos 99, Alicante 03080, Spain*

Corresponding author:

Meritxell Vilaseca

Address: Centre de Desenvolupament de Sensors, Instrumentació i Sistemes (CD6), Universitat Politècnica de Catalunya (UPC), Rambla Sant Nebridi 10, 08222 Terrassa, Barcelona (Spain)

Telephone number: +(34) 93 739 89 04

Fax number: +(34) 93 739 89 23

E-mail: mvilasec@oo.upc.edu

Abstract

We propose a luminance adaptation model (LAM) to increase the dynamic range of an imaging system when scenes containing areas of low and high illumination are imaged. The LAM that we developed is based on capturing images at different exposure times to obtain digital levels within the linear response zone for all the pixels in the image. The levels are subsequently transformed to a reference exposure time that is common to all pixels. We use a linear transformation whose coefficients are determined by the digital levels obtained for a set of flat-spectrum samples. In this study, the LAM is applied to a multispectral imaging system that is based on a CCD camera used for color measurements and spectral reconstructions. It is shown to be a very useful method for increasing the dynamic range of the system, whilst maintaining its accuracy.

Keywords: multispectral imaging, color measurement, charge-coupled device.

Introduction

Light in real-world scenes can vary widely, and therefore, they can have a high dynamic range. The limited dynamic range of digital cameras that are used to capture images leads to the loss of information in highly illuminated areas, where all light variations are mapped to the same value and thus become saturated, and in dimly illuminated areas, where information is overridden by sensor noise [1].

One way of overcoming this limitation is high dynamic range (HDR) imaging. The techniques applied in HDR imaging are based on capturing sequences of images of the same scene taken at different exposure conditions and by varying the exposure to control the light levels that are to be captured [2]. Sequences of images are acquired so that they can be merged into a single image with a higher dynamic range. Various techniques have been developed to estimate the underlying radiance values and build an accurate estimation of the values of the original scene from the HDR image [3-7]. This estimation is called a radiance map [1]. Nevertheless, the main aim of HDR imaging is image representation leading to a scene-referred representation of data, which contains enough information to achieve the desired appearance of the scene on a variety of output devices. It also provides a high quality device-independent input that exceeds the standards of traditional imaging, fully utilizes the capabilities of displays, and enhances the resulting image.

Like any other optoelectronic imaging sensors, imaging systems based on CCD cameras can be used as measuring instruments, for instance in colorimetric applications (color measurement) and multispectral applications (measurement of spectral features). In this case, the imaging conditions and/or setting parameters must be such that the system's response at each pixel is within the sensor's linear response zone, which is limited by the dynamic range of the

imaging system due to the background noise level and the pixels' saturation. However, in real scenes for a fixed exposure time, the digital responses for some of the pixels in the image are probably not located within the linear response zone of the imaging system, due to the large differences in radiance of the objects that are imaged.

The main purpose of the luminance adaptation model (LAM) proposed in this paper is to increase the dynamic range of a CCD camera-based imaging system used as an instrument for measuring color and spectral features of the imaged scene. The LAM is based on capturing images at different exposure times, to obtain digital levels that are within the linear response zone (useful digital levels) for all the pixels in the image. These levels are subsequently transformed to a reference exposure time that is common to all pixels [8] and [9]. We assess the LAM using two configurations of a CCD camera-based imaging system: a colorimetric configuration with 3 acquisition channels and a multispectral configuration with 7 acquisition channels.

The paper is structured as follows: first, we describe the basis of the Luminance Adaption Model (LAM) and its applications. Then, in the results section, we demonstrate the validity of the LAM when it is used with an imaging system for colorimetric and multispectral applications. Finally, in the last section, we present the most relevant conclusions of the study.

Luminance Adaptation Model (LAM)

The LAM proposed in this paper is based on capturing images at different exposure times to obtain digital levels that are within the linear response zone (useful digital levels, UDL) for all the pixels in the image. Given a specific scene, the useful digital level for each pixel and for each acquisition channel (i) can be expressed as follows:

$$UDL_i(t_{\exp}) = C \cdot t_{\exp} \int_{\lambda_{\min}}^{\lambda_{\max}} S(\lambda) \cdot L_e(\lambda) \cdot d\lambda \quad (1)$$

where C is a constant that basically depends on the irradiated area of the sensor, the f-number of the objective lens and its lateral magnification, t_{exp} is the exposure time used, $S(\lambda)$ is the spectral sensitivity of the acquisition channel, and $L_e(\lambda)$ is the radiance that comes from the scene. The former equation will be fulfilled for any radiance value of the acquired scene that provides a digital level within the linear response of the camera.

With the model that we developed, the useful digital levels for each acquisition channel at a certain exposure time are transformed to final digital levels at a reference exposure time (t_{ref}) that is common to all pixels. This is achieved by means of a linear transformation:

$$UDL_i(t_{ref}) = a_{it_{\exp}} \cdot UDL_i(t_{\exp}) + b_{it_{\exp}} \quad (2)$$

where $a_{it_{\exp}}$ and $b_{it_{\exp}}$ are the coefficients of the transformation for each acquisition channel and exposure time and are known as the LAM coefficients.

For each exposure time, the LAM coefficients are determined using a set of flat-spectrum samples, known as the calibration set, which contains the lightest and the darkest samples to be measured, i.e. a white sample and a black sample, and a range of samples whose luminance is uniformly distributed between the lightest and the darkest samples.

Hence, the LAM coefficients for each acquisition channel can be obtained by plotting the useful digital levels of the samples in the calibration set at each exposure time versus the corresponding useful digital levels at the reference exposure time and fitting them using a first-order least squares fitting.

Furthermore, to obtain the coefficients of the former transformation, different exposure times are measured for each acquisition channel and for the selected calibration set. The number

of exposure times considered and their scaling depend on the samples to be measured and, assuming that the system's noise has been corrected, on the bit depth of the imaging system, which determines the degree of discrimination between quite similar samples. The highest and lowest exposure times for each acquisition channel are selected so that the system's digital response to the darkest and lightest samples respectively in the calibration set are near the centre of the linear response zone of the imaging system. The intermediate exposure times should be selected so that at one exposure time or another, the system's digital responses to most of the samples are near the centre of the imaging system's linear response range. From all these exposure times and for each acquisition channel, the reference exposure time is selected as the one with the maximum number of samples in the calibration set, with digital levels within the system's linear response zone, i.e. at useful digital levels.

Once the LAM coefficients have been obtained for each exposure time considered for each acquisition channel, the LAM can be applied to the useful digital levels of any color samples captured by the imaging system. The final digital levels ($UDL_i(t_{ref})$) obtained from the LAM application with Equation (2) are not real digital levels, since they typically exceed the ($2^{bits} - 1$) level and increase the dynamic range of the imaging system. These digital levels are used to perform the color measurements and/or spectral reconstructions. Although they are not real, $UDL_i(t_{ref})$ allows all the samples to be mapped in the same exposure time, and therefore, they are comparable and useful for measurement purposes.

Finally, the LAM coefficients that are associated with a certain exposure time are specific for the light source used, as are the reference exposure time and the set of exposure times considered. Therefore, when the light source is changed, the LAM coefficients must be recalculated from the calibration set imaged at new exposure times.

The LAM proposed in this paper is completely general and applicable to any imaging system, whatever the number of acquisition channels.

LAM application

In this paper, the LAM is applied to an imaging system based on a QImaging QICAM Fast monochrome 1394 12-bit cooled CCD camera and an objective lens (Nikon AF Nikkor 28–105 mm), which allows color and spectral reflectance measurements to be made of the scene acquired from the digital levels of the image by means of multispectral tools [9-12]. Two configurations of this imaging system are considered: a colorimetric configuration with 3 acquisition channels, and a multispectral configuration with 7 acquisition channels [13].

The colorimetric configuration is obtained by inserting between the CCD camera and the objective lens a QImaging RGB-HM-NS tunable filter (Figure 1), which is controlled through the camera via software.

The multispectral configuration is obtained by inserting between the CCD camera and the objective lens a motorized filter wheel with seven CVI Laser interference filters covering the entire visible range of the spectrum and controlled by software. The interference filters used have peak positions or central wavelengths (CWLs) at 400 to 700 nm at 50 nm intervals. All of them have full widths at half maximums (FWHMs) of 40 nm, and their peak transmittances vary from 35% to 50%, depending on the CWL (Figure 2).

For the 12 bit CCD sensor used in this paper, the linear response zone (in which the channels' response is a linear function of the exposure) is located between the 330 and 3700 digital levels, which establish the useful dynamic range of the imaging system (Figure 3).

The LAM coefficients are determined using the neutral patches in the Munsell Book of Color – Matte Collection as a calibration set. These patches are placed inside a light booth with a D65 daylight simulator.

For each acquisition channel, the reference exposure time is selected so that the digital levels associated with all of Munsell's neutral patches are within the linear response zone of the system, i.e. are useful digital levels. In addition to the reference exposure time, a set of other exposure times are considered for each acquisition channel.

Once the coefficients have been obtained for each exposure time considered for each acquisition channel, the LAM is applied to the imaging system with the two configurations described. Specifically, in this study we measured the color and the spectral reflectance corresponding to the useful digital levels of the color patches of the GretagMacbeth ColorChecker DC chart (CCDC) and the GretagMacbeth ColorChecker Color Rendition chart (CCCR) placed inside the same light booth as the calibration set. As mentioned above, the system allows us to obtain colorimetric and spectral information on the acquired scene by means of multispectral tools, which include the use of matrices to transform the measured digital levels into colorimetric or spectral data. Transformation matrices can be computed using a training set of samples, whose digital levels besides the reflectance spectra are known a priori. In this study, the following methods are used for the color measurements and spectral reconstructions from the system's digital responses: the pseudoinverse method [10] and [14-17] for the colorimetric configuration, and the principal component analysis method [10], [11], [14], [16] and [18] for the multispectral configuration. The imaging system was trained using the final digital levels resulting from the LAM application, as well as the reflectance spectra of the CCDC and CCCR color samples. The same groups of samples are used to test the accuracy of the system's

performance with and without the LAM application, since there is a certain exposure time at which useful digital levels for all color patches are obtained for these charts. All possible combinations of the CCDC and CCCR charts as training and test sets are evaluated. The accuracy of the color measurement is evaluated in terms of the CIELAB color difference, and the accuracy of the spectral reconstruction is evaluated in terms of the root mean square error (RMSE).

Results

Colorimetric Configuration

The LAM coefficients obtained for the R, G and B acquisition channels of the colorimetric configuration are presented in Table 1. The reference exposure time chosen for each acquisition channel is highlighted.

Figure 4 shows an example of the first order least squares fitting applied to the digital levels of the same Munsell's neutral patches at the reference exposure time and at an exposure time of 30 ms for the three acquisition channels of the colorimetric configuration.

The accuracy of the system's performance when the LAM is used for all possible combinations of the CCDC and the CCCR charts as training and test sets is compared with the corresponding accuracy of the system's performance without the LAM, when the digital levels are used directly for all color patches of the CCDC and the CCCR charts obtained from images taken at the reference exposure times for the R, G and B channels. These exposure times are such that the digital levels associated with all color samples of both the CCDC and the CCCR charts are useful.

The application of the LAM does not worsen the accuracy of the system's color measurements. In fact, it slightly improves color measurement performance for all combinations of the CCDC and the CCCR charts used as training and test sets (Table 2).

The application of the LAM slightly improves the accuracy of the system's spectral reconstruction performance for all combinations of the CCDC and the CCCR charts used as training and test sets (Table 3). The improvement in accuracy is very similar for all combinations of the CCDC and the CCCR charts used as training and test sets.

Multispectral Configuration

Table 4 presents the LAM coefficients associated with the different exposure times considered for each acquisition channel of the multispectral configuration. The reference exposure time chosen for each acquisition channel is highlighted.

Once we know the LAM coefficients associated with each exposure time for the seven acquisition channels of the imaging system, we can follow the same procedure as that used for the colorimetric configuration. Very similar results are obtained with and without the application of the LAM for all combinations of the CCDC and the CCCR charts used as training and test sets, in terms of the accuracy of color measurement (Table 5) and spectral reconstruction (Table 6).

Conclusions

A luminance adaptation model (LAM) has been proposed to increase the dynamic range of an imaging system used as a measuring instrument, which is limited by the useful (linear) dynamic range of the CCD camera used. This model is based on capturing images at different exposure

times, to obtain useful digital levels for all the pixels in the image. These levels are subsequently transformed to a reference exposure time that is common to all pixels.

The LAM has been applied to a multispectral imaging system based on a CCD camera and used for color measurements and spectral reconstructions. It has been proved to be a very useful method for increasing the dynamic range of the system and maintaining its accuracy. It is suitable mainly for images that have zones with an outstandingly wide range of light variations, in order to make all zones of the image useful for color measurement or for spectral reconstruction. The LAM proposed in this paper is completely general and applicable to any imaging system, whatever the number of acquisition channels.

Acknowledgments

This research was supported by the Spanish Ministry of Education and Science; grant number DPI2008-06455-C02-01. M. de Lasarte would like to thank the Spanish Ministry of Education and Science for the Ph.D. grant she received.

References

[1] S. Battiato, A. Castorina, M. Mancuso, High dynamic range imaging for digital still camera: an overview, J Electron. Imaging 12 (2003) 459–469.

[2] R. Mantiuk, G. Krawczyka, R. Mantiuk, H. P. Seidela, High dynamic range imaging pipeline: perception-motivated representation of visual content, in Proceedings of the SPIE 6492, 2007, pp. 6492/1-6492/12.

[3] P. E. Debevec, J. Malik, Recovering high dynamic range radiance maps from photographs, in Proceedings of the 24th Annual Conference on Computer Graphics and Interactive Techniques, ACM Press/Addison-Wesley Publishing Co. New York, USA, 1997, pp. 369-378.

[4] T. Mitsunaga, S. K. Nayar, Radiometric self calibration, in Proceedings of IEEE Conference on Vision and Pattern Recognition, IEEE, 1999, pp. 374-380.

[5] S. Mann, R. W. Picard, Being 'undigital' with digital cameras: Extending dynamic range by combining differently exposed pictures, in Proceedings of IS&T 46th Annual Conference, The Society for Imaging Science and Technology, Springfield, VA, 1995, pp. 422-428.

[6] S. Mann, Comparametric equations with practical applications in quantigraphic image processing, IEEE Trans. Image Process. 9 (2000) 1389-1406.

[7] S. K. Nayar, T. Mitsunaga, High dynamic range imaging: spatially varying pixel exposures, in Proceedings of IEEE Conference on Vision and Pattern Recognition, IEEE, 2000, pp. 472-479.

[8] J. Pujol, M. de Lasarte, M. Vilaseca, M. Arjona, High dynamic range multispectral system for wide color gamut measurements, in Proceedings of the Third European Conference on Color in Graphics, Imaging and Vision, The Society for Imaging Science and Technology, Springfield, VA, 2006, pp. 404-409.

[9] M. Vilaseca, J. Pujol, M. Arjona, M. de Lasarte, Multispectral system for the reflectance reconstruction in the near-infrared region, Appl. Opt. 45 (2006) 4241-4253.

[10] M. de Lasarte, M. Vilaseca, J. Pujol, M. Arjona, Color measurements with colorimetric and multispectral imaging systems, in Proceedings of the SPIE 6062, 2006, pp. 0F1-0F11.

[11] J. Y. Hardeberg, F. Schmitt, H. Brettel, Multispectral color image capture using a liquid crystal tunable filter, Opt. Eng. 40 (2002) 2532-2548.

[12] D. Connah, A. Alsam, J. Y. Hardeberg, Multispectral imaging: how many sensors do we need?, J. Imaging Sci. Technol. 50 (2006) 45-52.

[13] M. Vilaseca, R. Mercadal, J. Pujol, M. Arjona, M. de Lasarte, R. Huertas, M. Melgosa, F. H. Imai, Characterization of the human iris spectral reflectance with a multispectral imaging system, Appl. Opt. 47 (2008) 5622-5630.

[14] J. Y. Harderberg, Acquisition and reproduction of color images: colorimetric and multispectral approaches, Ph.D. thesis, École Nationale Supérieur des Télécommunications, Paris, 1999.

[15] A. Ribés, F. Schmitt, H. Brettel, Reconstructing spectral reflectances of oil pigments with neural networks, in Proceedings of the Third International Conference on Multispectral Color Science, M. Hauta-Kasari, J. Hiltunen, J. Vanhanen eds., Joensuu, Finland, 2001, pp. 9-12.

[16] F. H. Imai, L.A. Taplin, E. A. Day, Comparison of the accuracy of various transformations from multi-band images to reflectance spectra, Technical report (Munsell Color Science Laboratory, 2002),

https://ritdml.rit.edu/dspace/bitstream/1850/4356/1/LTaplinTechReport2002.pdf

[17] Y. Zhao, L. A. Taplin, M. Nezamabadi, R. S. Berns, Methods of spectral reflectance reconstruction for a Sinarback 54 digital camera, Technical report (Munsell Color Science Laboratory, 2004), http://www.art-si.org/PDFs/Acquisition/Sinar_Spectral_Est_2004.pdf

[18] F. H. Imai, R. S. Berns, Comparative analysis of spectral reflectance reconstruction in various spaces using a trichromatic camera system, J. Imaging Sci. Technol. 44 (2000) 280-287.

Figure caption listing page

Fig. 1. Relative spectral sensitivities of the channels used in the colorimetric configuration of the imaging system (RGB tunable filter and CCD camera).

Fig. 2. Transmittance spectra of the interference filters used in the multispectral configuration of the imaging system. Interference filters are named by their central wavelength.

Fig. 3. Mean digital level versus exposure time (ms) when a uniform radiance field is imaged with the QImaging QICAM CCD camera.

Fig. 4. An example of the first order least squares fitting applied to the digital levels of the same Munsell's neutral patches at the reference exposure time and at an exposure time of 30 ms, for the (a) R, (b) G and (c) B acquisition channels of colorimetric configuration. Each point in the plot represents a Munsell's neutral patch.

Table title listing page

Table 1: Colorimetric configuration: LAM coefficients associated with each exposure time (t_{exp}) considered for the R, G, and B channels of the colorimetric configuration. The reference exposure time (t_{ref}) chosen for each acquisition channel is highlighted.

Table 2: Colorimetric configuration: comparison between the mean, minimum, maximum and standard deviation of the CIELAB color difference values obtained with (LAM) and without (NO LAM) the application of the Luminance Adaptation Model, for all combinations of the CCDC and CCCR charts used as training and test sets.

Table 3: Colorimetric configuration: comparison between the mean, minimum, maximum and standard deviation of the RMSE values obtained with (LAM) and without (NO LAM) the application of the Luminance Adaptation Model, for all combinations of the CCDC and CCCR charts used as training and test sets.

Table 4: Multispectral configuration: LAM coefficients associated with each exposure time (texp) considered for the 7 channels of the multispectral configuration. Each acquisition channel is denoted by the central wavelength of the interference filter F. The reference exposure time (tref) chosen for each acquisition channel is highlighted.

Table 5: Multispectral configuration: comparison between the mean, minimum, maximum and standard deviation of the CIELAB color difference values obtained with (LAM) and without (NO LAM) the application of the Luminance Adaptation Model, for the different combinations of the CCDC and CCCR charts used as training and test sets.

Table 6: Multispectral configuration: comparison between the mean, minimum, maximum and standard deviation of the RMSE values obtained with (LAM) and without (NO LAM) the

application of the Luminance Adaptation Model, for the different combinations of the CCDC and CCCR charts used as training and test sets.

Tables

Table 1: Colorimetric configuration: LAM coefficients associated with each exposure time (t_{exp}) considered for the R, G, and B channels of the colorimetric configuration. The reference exposure time (t_{ref}) chosen for each acquisition channel is highlighted.

R CHANNEL			
t_{exp} (ms)	*a*	*b*	r^2
10	1.97	-134.03	0.9992
20	1.00	0.00	1.0000
30	0.66	38.13	0.9999
40	0.51	61.63	0.9996
50	0.41	76.21	0.9992
60	0.35	87.38	0.9988
70	0.30	92.84	0.9986
80	0.26	98.96	0.9984
90	0.23	102.54	0.9983
100	0.21	106.80	0.9981

G CHANNEL			
t_{exp} (ms)	*a*	*b*	r^2
10	1.98	-135.91	0.9992
20	1.00	0.00	1.0000
30	0.69	37.71	0.9999
40	0.51	62.20	0.9996
50	0.41	76.76	0.9992
60	0.35	85.40	0.9989
70	0.30	92.98	0.9986
80	0.26	100.52	0.9983
90	0.23	103.73	0.9981
100	0.21	106.64	0.9980

B CHANNEL			
t_{exp} (ms)	*a*	*b*	r^2
10	3.96	-429.62	0.9963
20	1.98	-138.95	0.9991
30	1.35	-47.23	0.9999
40	1.00	0.00	1.0000
60	0.68	39.68	0.9999
80	0.51	63.23	0.9996
100	0.41	78.21	0.9992
120	0.34	89.12	0.9987
140	0.29	96.51	0.9983
160	0.25	101.16	0.9980

Table 2: Colorimetric configuration: comparison between the mean, minimum, maximum and standard deviation of the CIELAB color difference values obtained with (LAM) and without (NO LAM) the application of the Luminance Adaptation Model, for all combinations of the CCDC and CCCR charts used as training and test sets.

ΔE^*_{ab} – NO LAM				
Training	**CCDC**	**CCDC**	**CCCR**	**CCCR**
Test	**CCDC**	**CCCR**	**CCCR**	**CCDC**
mean	5.02	7.26	6.05	5.19
minimum	0.55	0.91	0.55	0.65
maximum	17.14	19.1	17.2	14.89
std. dev.	3.55	5.23	4.76	3.01

ΔE^*_{ab} – LAM				
Training	**CCDC**	**CCDC**	**CCCR**	**CCCR**
Test	**CCDC**	**CCCR**	**CCCR**	**CCDC**
mean	3.60	5.28	4.06	3.86
minimum	0.35	2.23	0.56	0.67
maximum	10.34	11.15	9.03	11.12
std. dev.	2.31	2.64	2.44	2.11

Table 3: Colorimetric configuration: comparison between the mean, minimum, maximum and standard deviation of the RMSE values obtained with (LAM) and without (NO LAM) the application of the Luminance Adaptation Model, for all combinations of the CCDC and CCCR charts used as training and test sets.

RMSE – NO LAM				
Training	**CCDC**	**CCDC**	**CCCR**	**CCCR**
Test	**CCDC**	**CCCR**	**CCCR**	**CCDC**
mean	4.58E-02	5.80E-02	5.30E-02	5.35E-02
minimum	1.39E-02	3.16E-02	2.35E-02	1.69E-02
maximum	17.16E-02	17.17E-02	16.24E-02	16.29E-02
std. dev.	2.23E-02	2.89E-02	2.70E-02	2.38E-02

RMSE – LAM				
Training	**CCDC**	**CCDC**	**CCCR**	**CCCR**
Test	**CCDC**	**CCCR**	**CCCR**	**CCDC**
mean	4.26E-02	5.51E-02	5.05E-02	5.08E-02
minimum	1.17E-02	3.02E-02	2.46E-02	1.43E-02
maximum	17.57E-02	17.54E-02	16.42E-02	16.50E-02
std. dev.	2.38E-02	3.12E-02	2.82E-02	2.45E-02

Table 4: Multispectral configuration: LAM coefficients associated with each exposure time (texp) considered for the 7 channels of the multispectral configuration. Each acquisition channel is denoted by the central wavelength of the interference filter F. The reference exposure time (tref) chosen for each acquisition channel is highlighted.

CHANNEL F400			
t_{exp} (ms)	*a*	*b*	r^2
300	1.64	-81.87	0.9998
400	1.24	-28.47	1.0000
500	1.00	0.00	1.0000
750	0.68	35.29	0.9999
1000	0.51	54.82	0.9998
1250	0.41	70.07	0.9997
1500	0.34	77.99	0.9996

CHANNEL F450			
t_{exp} (ms)	*a*	*b*	r^2
25	1.97	-138.24	0.9990
50	1.00	0.00	1.0000
75	0.68	39.02	0.9999
100	0.51	61.51	0.9996
200	0.26	99.51	0.9984
250	0.21	105.58	0.9982
300	0.17	111.63	0.9982

CHANNEL F500			
t_{exp} (ms)	*a*	*b*	r^2
20	1.48	-63.26	0.9998
30	1.00	0.00	1.0000
40	0.76	26.23	1.0000
60	0.51	60.07	0.9997
100	0.31	88.79	0.9990
150	0.21	104.43	0.9987
200	0.15	115.01	0.9987

CHANNEL F550			
t_{exp} (ms)	*a*	*b*	r^2
10	1.97	-136.05	0.9992
20	1.00	0.00	1.0000
30	0.68	38.26	0.9999
50	0.41	76.28	0.9992
100	0.21	106.67	0.9980
125	0.17	113.24	0.9979
150	0.14	119.44	0.9979

CHANNEL F600			
t_{exp} (ms)	*a*	*b*	r^2
10	1.96	-136.56	0.9991
20	1.00	0.00	1.0000
30	0.67	40.60	0.9999
50	0.41	76.61	0.9992
100	0.21	106.47	0.9980
125	0.16	114.13	0.9978
150	0.14	118.58	0.9978

CHANNEL F650			
t_{exp} (ms)	*a*	*b*	r^2
10	2.96	-286.20	0.9971
20	1.49	-69.33	0.9996
30	1.00	0.00	1.0000
50	0.61	50.64	0.9997
100	0.31	93.17	0.9981
125	0.24	104.06	0.9971
150	0.21	108.37	0.9967

CHANNEL F700			
t_{exp} (ms)	*a*	*b*	r^2
25	5.93	-722.71	0.9943
50	3.00	-286.46	0.9972
75	2.00	-140.47	0.9991
100	1.50	-68.75	0.9997
150	1.00	0.00	1.0000
200	0.76	29.73	0.9999
300	0.52	60.66	0.9996

Table 5: Multispectral configuration: comparison between the mean, minimum, maximum and standard deviation of the CIELAB color difference values obtained with (LAM) and without (NO LAM) the application of the Luminance Adaptation Model, for the different combinations of the CCDC and CCCR charts used as training and test sets.

ΔE^*_{ab} – NO LAM				
Training	**CCDC**	**CCDC**	**CCCR**	**CCCR**
Test	**CCDC**	**CCCR**	**CCCR**	**CCDC**
mean	3.35	5.46	3.83	3.76
minimum	0.10	1.09	0.49	0.48
maximum	12.12	21.65	12.45	10.41
std. dev.	2.56	4.50	3.20	2.19

ΔE^*_{ab} – LAM				
Training	**CCDC**	**CCDC**	**CCCR**	**CCCR**
Test	**CCDC**	**CCCR**	**CCCR**	**CCDC**
mean	3.35	5.43	3.81	3.82
minimum	0.12	1.08	0.44	0.52
maximum	11.63	20.95	11.98	10.35
std. dev.	2.49	4.32	3.12	2.03

Table 6: Multispectral configuration: comparison between the mean, minimum, maximum and standard deviation of the RMSE values obtained with (LAM) and without (NO LAM) the application of the Luminance Adaptation Model, for the different combinations of the CCDC and CCCR charts used as training and test sets.

RMSE – NO LAM				
Training	**CCDC**	**CCDC**	**CCCR**	**CCCR**
Test	**CCDC**	**CCCR**	**CCCR**	**CCDC**
mean	3.05E-02	4.59E-02	3.06E-02	4.06E-02
minimum	0.85E-02	2.45E-02	1.29E-02	1.22E-02
maximum	10.55E-02	7.25E-02	6.56E-02	10.63E-02
std. dev.	1.28E-02	1.26E-02	1.50E-02	2.22E-02

RMSE – LAM				
Training	**CCDC**	**CCDC**	**CCCR**	**CCCR**
Test	**CCDC**	**CCCR**	**CCCR**	**CCDC**
mean	3.03E-02	4.56E-02	3.04E-02	4.05E-02
minimum	0.82E-02	2.28E-02	1.40E-02	1.29E-02
maximum	10.31E-02	7.42E-02	6.62E-02	10.54E-02
std. dev.	1.26E-02	1.31E-02	1.44E-02	2.18E-02

Figures

Fig. 1. Relative spectral sensitivities of the channels used in the colorimetric configuration of the imaging system (RGB tunable filter and CCD camera).

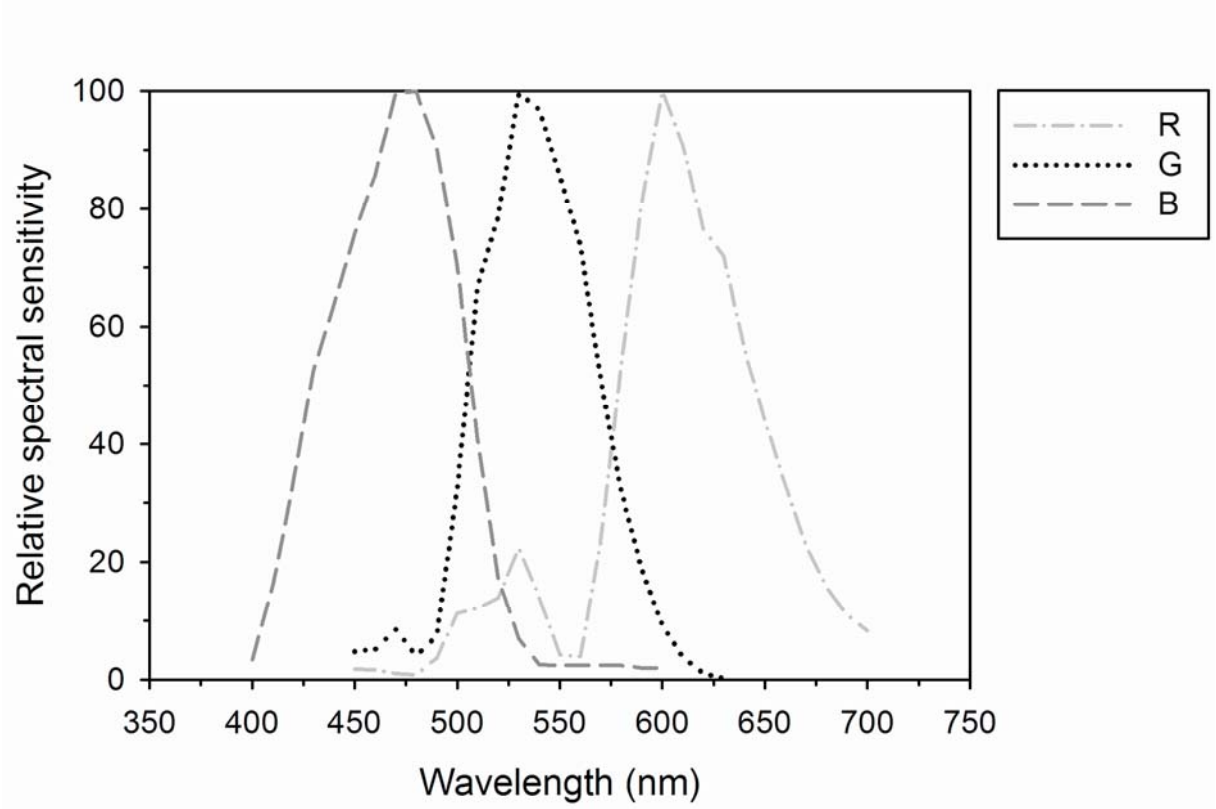

Fig. 2. Transmittance spectra of the interference filters used in the multispectral configuration of the imaging system. Interference filters are named by their central wavelength.

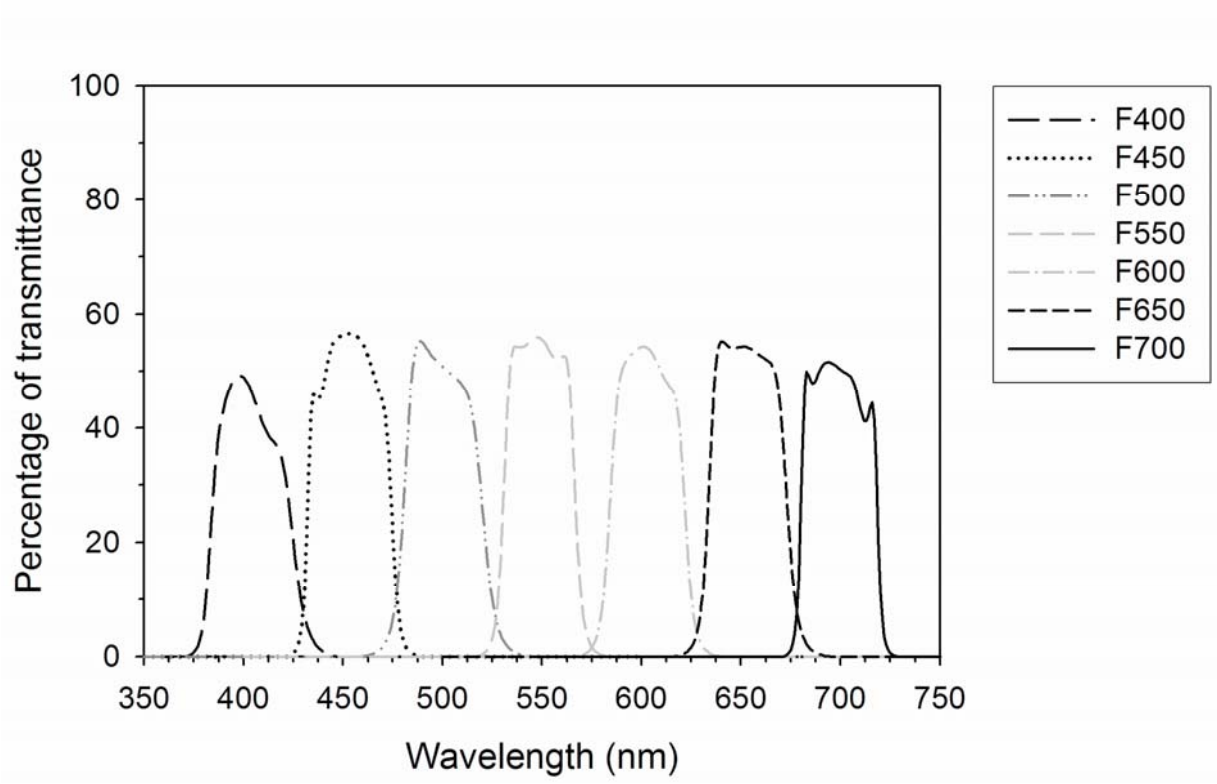

Fig. 3. Mean digital level versus exposure time (ms) when a uniform radiance field is imaged with the QImaging QICAM CCD camera: linear scale (a) and logarithmic scale (b).

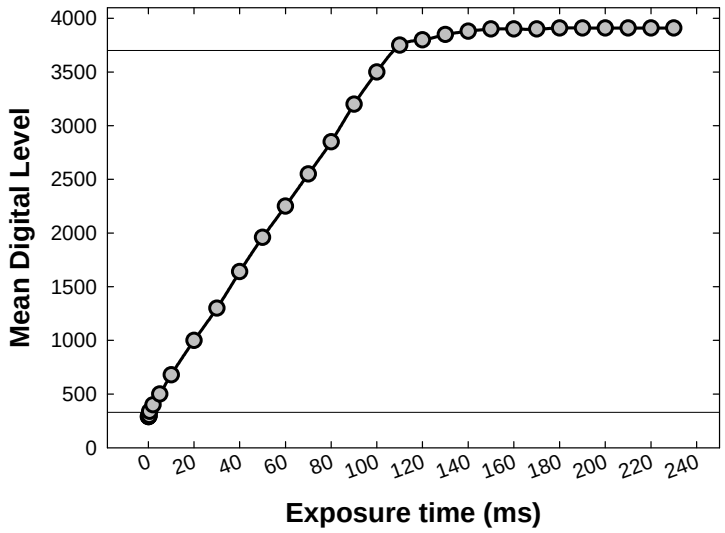

(a)

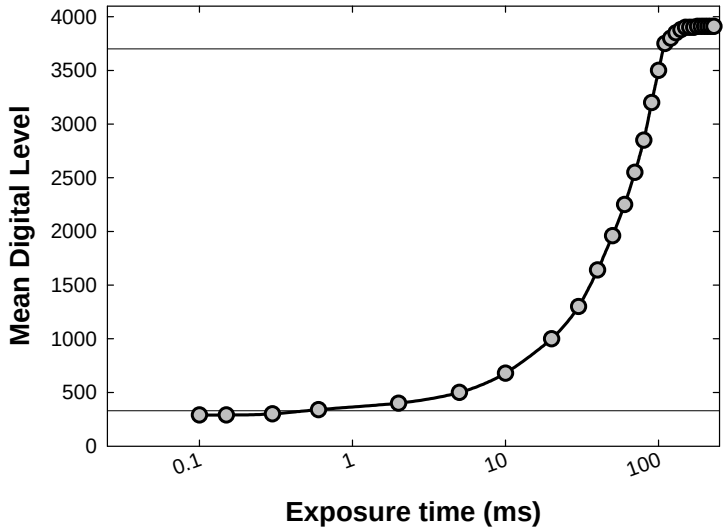

(b)

Fig. 4. An example of the first order least squares fitting applied to the digital levels of the same Munsell's neutral patches at the reference exposure time and at an exposure time of 30 ms, for the (a) R, (b) G and (c) B acquisition channels of the colorimetric configuration. Each point in the plot represents a Munsell's neutral patch.

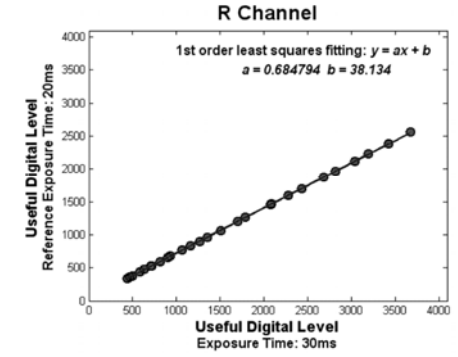

(a)

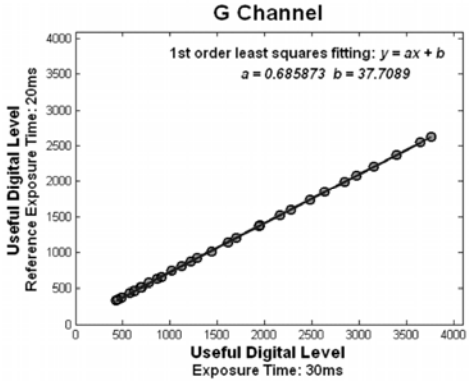

(b)

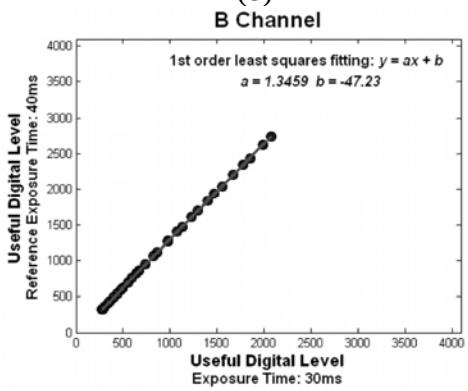

(c)